Optimization of the thermodynamic model of a solar driven Aqua - ammonia absorption refrigeration system

J. ABDULATEEF, K.SOPIAN, M.YAHYA, A. ZAHARIM and M. ALGHOUL
Solar Energy Research Institute (SERI)
University Kebangsaan Malaysia
43600 Bangi, Selangor
MALAYSIA

Abstract: - The aim of this study is to simulate a solar single effect ammonia-water absorption refrigeration system. The influences of operating conditions and effectiveness of heat exchanger on the thermal loads of components, coefficients of performance(COPc, COP) and efficiency ratio (η) are investigated. It is concluded that the COPc and COP values increase with increasing generator and evaporator temperatures but decrease with increasing condenser and absorber temperatures. The (η) value varies with these temperatures. Also, the effectiveness of heat exchanger determines the maximum temperature that can be used in order to obtain the maximum COP out of the system.

Key -Words: Efficiency ratio; effectiveness; performance parameters; solar refrigeration

1 Introduction

During recent years, research aimed at the development of technologies that can offer reductions in energy consumption, peak electrical demand and energy costs without lowering the desired level of comfort conditions has intensified. By reason that solar refrigeration technologies have the advantage of removing the majority of harmful effects of traditional refrigeration machines and that the peaks of requirements in cold coincide most of the time with the availability of the solar radiation, the development of solar refrigeration technologies became the worldwide focal point for concern again. Theoretical and experimental studies have been conducted and reported by various authors to optimize the performance of absorption refrigeration cycles using NH_3-H_2O as refrigerant-absorbent.

Sierra et al. [1] used a solar pond to power an intermittent absorption refrigerator with NH_3-H_2O solution. It is reported that generation temperatures as high as 73 ^oC and evaporation temperatures as low as –2 ^oC could be obtained. The thermal COP working under such conditions was in the range of 0.24-0.28.

Bulgan [2] optimized an aqua-ammonia absorption refrigeration system (ARS) in the light of the first law of thermodynamics. A theoretical model was developed for the ARS. The coefficient of performance (COP) was maximized for various evaporator, condenser and absorber temperatures. Sun [3] performed a thermodynamic analyses of different binary mixtures considered in absorption refrigeration cycle, and the performances were compared. Srikhirin et al. [4] presented a literature review on absorption refrigeration technology such as various types of absorption refrigeration systems, researches on working fluids and improvement of absorption processes. Ben Ezzine et al. [5] presented the modelling, thermodynamic simulation and Second Law analysis of an ammonia-water double-effect, double generator absorption chiller. Results indicated that the absorber, solution heat exchangers, and condenser have the most potential to improve chiller efficiency. In the study of Abdulateef et al. [6], the thermodynamic properties of ammonia based binary mixtures (NH_3-H_2O, NH_3-$LiNO_2$, NH_3-NaSCN) were given, and the performances of the cycles were compared.

In the present study, a parametric thermodynamic analysis of a single stage solar absorption refrigeration system is performed. Coefficients of system performance (COPc, COP) and efficiency ratio (η) are compared at various operating temperatures. The influence of heat exchanger effectiveness on the thermal loads of components, solution temperatures and performance parameters are also investigated.

2 Cycle description

Fig.1 shows the schematic diagram of the solar driven aqua-ammonia absorption refrigeration cycle. High-pressure liquid refrigerant (2) from the condenser passes into the evaporator (4) through an expansion valve (3) that reduces the pressure of the refrigerant to the low pressure existing in the evaporator. The liquid refrigerant (3) vaporizes in the evaporator by absorbing heat from the material being cooled and the resulting low-pressure vapor (4) passes to the absorber, where it is absorbed by the strong solution coming from the generator (8) through an expansion valve (10), and forms the weak solution (5). The weak solution (5) is pumped to the generator pressure (7). Heat from a high-temperature source by solar energy used in the generator to separate the binary solution of water and ammonia by causing ammonia to vaporize. The remaining solution (8) flows back to the absorber and, thus, completes the cycle. By weak solution (strong solution) is meant that the ability of the solution to absorb the refrigerant vapor is weak (strong), according to the ASHRAE definition [7]. For the current study, it is assumed that the refrigerant vapor leaving the generator is 100% ammonia. In order to improve cycle performance, a solution heat exchanger is normally added to the cycle, it is an energy saving component.

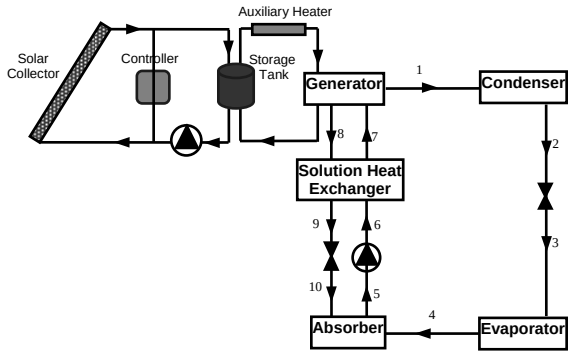

Fig. 1. Solar absorption refrigeration system

For the generator, the mass and energy balances yield:

$$\dot{m}_7 = \dot{m}_1 + \dot{m}_8 \quad (1)$$

$$\dot{m}_7 X_7 = \dot{m}_1 X_1 + \dot{m}_8 X_8 \quad (2)$$

The flow rates of the weak and strong solutions can be determined from equations (1) and (2), respectively:

$$\dot{m}_7 = \frac{X_1 - X_8}{X_7 - X_8}\dot{m}_1 \quad (3)$$

$$\dot{m}_8 = \frac{X_1 - X_7}{X_7 - X_8}\dot{m}_1 \quad (4)$$

The circulation ratio (CR) can be defined as:

$$CR = \frac{\dot{m}_7}{\dot{m}_1} \quad (5)$$

The components' thermal loads of the ARS are expressed as follows:

$$Q_{gen} = \dot{m}_1 h_1 + \dot{m}_8 h_8 - \dot{m}_7 h_7 \quad (6)$$

$$Q_{abs} = \dot{m}_4 h_4 + \dot{m}_{10} h_{10} - \dot{m}_5 h_5 \quad (7)$$

$$Q_{cond} = \dot{m}_1 (h_1 - h_2) \quad (8)$$

$$Q_{evp} = \dot{m}_1 (h_4 - h_3) \quad (9)$$

The energy balance for the solution heat exchanger is as follows:

$$T_9 = \varepsilon_{SHE} T_6 + (1 - \varepsilon_{SHE}) T_8 \quad (10)$$

$$h_7 = h_6 + \frac{\dot{m}_8}{\dot{m}_6}(h_8 - h_9) \quad (11)$$

The pump work for the weak solution leaving the absorber may be expressed as:

$$h_6 = h_5 + (P_6 - P_5) v_6 \quad (12)$$

$$W_{me} = (P_6 - P_5) v_6 \quad (13)$$

The system performance is measured by the coefficient of performance (COP):

$$COP = \frac{Q_{evp}}{Q_{gen} + W_{me}} \quad (14)$$

The efficiency ratio (η) is defined as the ratio of the coefficient of performance to the Carnot coefficient of performance (COPc). The Carnot coefficient of performance is the maximum possible coefficient of performance of an ARS under given operating conditions.

$$COP_c = \left(\frac{T_{gen} - T_{abs}}{T_{gen}}\right).\left(\frac{T_{evp}}{T_{cond} - T_{evp}}\right) \quad (15)$$

$$\eta = \frac{COP}{COP_C} \quad (16)$$

The performance increase ratio (PIR) of the system using heat exchanger is expressed as follows:

$$PIR = \frac{COP_2 - COP_1}{COP_1} \quad (17)$$

Where COP_1 is the coefficient of performance without heat exchanger ($\varepsilon_{SHE} = 0$) and COP_2 is the coefficient of performance with heat exchanger ($\varepsilon_{SHE} > 0$).

3 Solution properties

3.1. Refrigerant NH_3

In the usual ranges of pressure and temperature concerning refrigeration applications, the two

phase equilibrium pressure and temperature of the refrigerant NH_3 are linked by the relation:

$$P(T) = 10^3 \sum_{i=0}^{6} a_i (T - 273.15)^i \quad (18)$$

The specific enthalpies of saturated liquid and vapor NH_3 are expressed in terms of temperature as follows:

$$h_l(T) = \sum_{i=0}^{6} b_i (T - 273.15)^i \quad (19)$$

$$h_v(T) = \sum_{i=0}^{6} c_i (T - 273.15)^i \quad (20)$$

All coefficients of equations above are listed by Sun [3].

3.2. NH_3-H_2O solution

The relation between saturation pressure and temperature of an ammonia-water mixture is given as:

$$LogP = A - \frac{B}{T} \quad (21)$$

Where:

$$A = 7.44 - 1.767X + 0.982X^2 + 0.362X^3 \quad (22)$$

$$B = 2013.8 - 2155.7X + 1540.9X^2 - 194.7X^3 \quad (23)$$

The relation among temperature, concentration and enthalpy is as follows:

$$h(T, \overline{X}) = 100 \sum_{i=1}^{16} a_i \left(\frac{T}{273.16} - 1\right)^{mi} \overline{X}^{ni} \quad (24)$$

where $\overline{X}$ is the ammonia mole fraction and is given as follows:

$$\overline{X} = \frac{18.015X}{18.015X + 17.03(1 - X)} \quad (25)$$

The relation among specific volume, temperature and concentration is given as:

$$v(T, X) = \sum_{j=0}^{3} \sum_{i=0}^{3} a_{ij} (T - 273.15)^i X^j \quad (26)$$

All coefficients of equations above are listed by Sun [3].

4 Results and discussion

4.1. The effects of operating temperatures

The effects of the generator, evaporator and condenser temperatures on the thermal loads of the components are shown in Figs. 2-4. In these calculations, the operating temperatures ranges are selected as follows: T_{gen}=70-120 ^oC, T_{evp}=-20-10 ^oC, T_{cond}=10-45 ^oC, T_{abs}=25 ^oC, ε_{SHE}= 50 % and refrigerant mass flow rate $\dot{m}_1 = 0.0166$ Kg/sec.

As it can be seen from Fig. 2, when the generator temperature increases, the generator and absorber thermal loads (Q_{gen} and Q_{abs}) decrease. If the generator temperature gets higher, the concentration of the solution leaving the generator decrease, and hence, the CR decreases, as can be seen from equations (3)-(5). Moreover, the weak solution temperature and, hence, the enthalpy (h_7) is increased by the strong solution in the SHE. The generator thermal load is decreased by both decreasing the CR and increasing h_7. The enthalpy of the ammonia vapor (h_1) leaving the generator decreases with increasing generator temperature, and hence, condenser thermal load (Q_{cond}) decreasing from 19.293 kW to 16.896 kW.

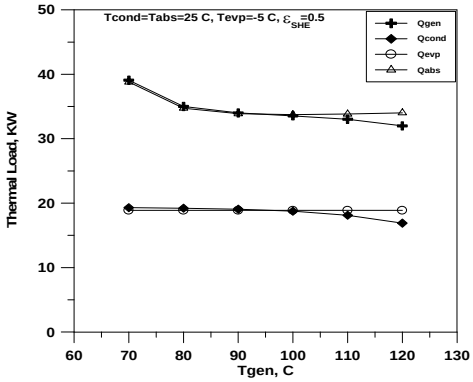

Fig. 2. Variation of thermal loads with the generator temperature

The evaporator thermal load does not change with generator temperature and remains as a constant value of 18.882 KW. The evaporator temperature affects the low pressure of the system. If the evaporator temperature rises, the concentration of the weak solution increase while the CR decrease. They cause a decrease in the absorber thermal load; on the other hand, the decreasing of CR decreases the generator thermal load (Fig. 3). A small increase in evaporator outlet enthalpy (h_4) also causes a small amount of increase in the evaporator thermal load (from 18.522 kW to 19.32 kW). The condenser thermal load remains unchanged as 19.059 kW.

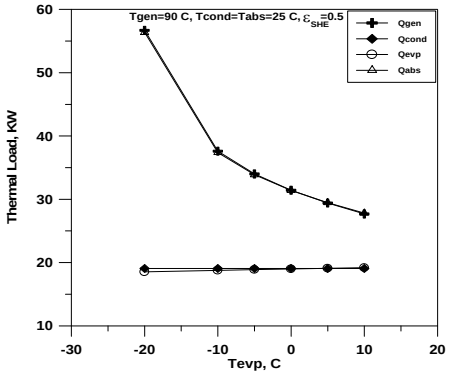

Fig. 3. Variation of thermal loads with the evaporator temperature

The high pressure of the system increases, and the concentration of the strong solution increases when the condenser temperature increases. With increasing strong solution concentration, the CR increases, and in this case, the thermal loads of both the generator and absorber increase (Fig. 4). The enthalpy of the saturated liquid (h_2) leaving the condenser increases with increasing condenser temperature. Thus, it causes a small amount of decrease in the condenser and evaporator thermal loads.

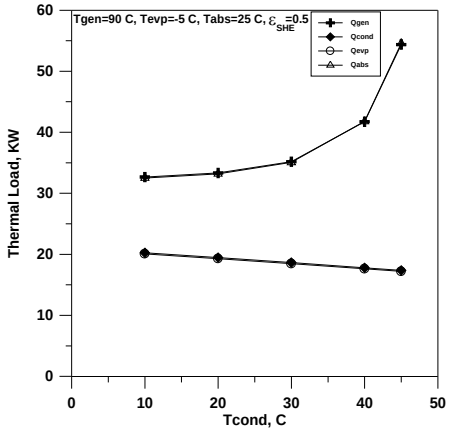

Fig. 4. Variation of thermal loads with the condenser temperature

The variations of the coefficients of performance (COPc and COP) and efficiency ratio (η) with operating temperatures are given in Figs. 5-7. The high COPc and COP values are obtained at high generator and evaporator temperatures (Figs. 6 and 7). As is seen from the equation (15), the performance of the Carnot cycle gets better with increasing generator and evaporator temperatures. Since the increase in COPc is faster than that in COP, the η value gradually decreases.

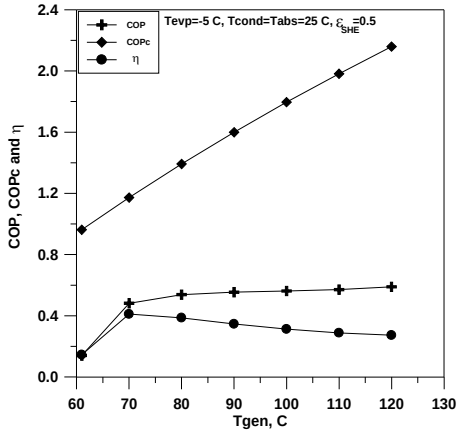

Fig. 5. Variation of performance parameters with the generator temperature

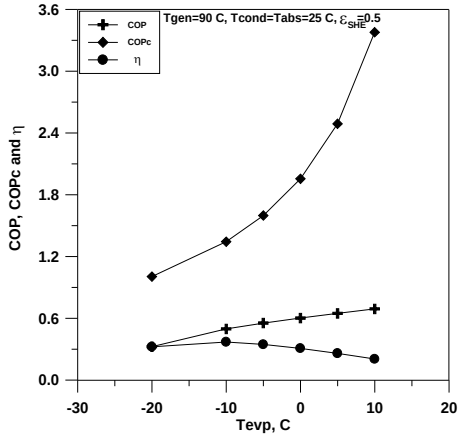

Fig. 6. Variation of performance parameters with the evaporator temperature

It is seen from Fig. 7, that the COPc and COP values decrease with increasing condenser temperature. When the temperatures of the condenser increase, the thermal load of the generator rises, and the performance of the system gets worse. While the η value increases with increasing the condenser temperature up to 40 ^{o}C, it decreases above 40 ^{o}C due to the relatively rapid decrease of COP.

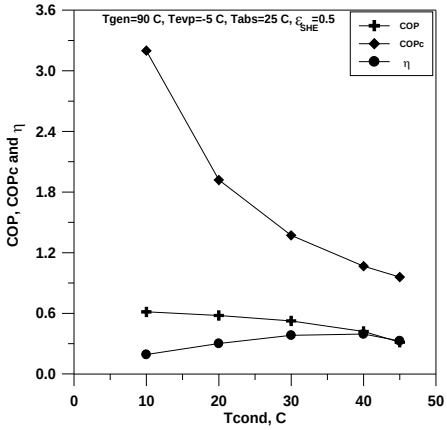

Fig. 7. Variation of performance parameters with the condenser temperature

The effect of absorber temperature is similar to that of condenser temperature. The generally speaking, the condenser and absorber temperatures should be at a similar level.

4.2. The effects of solution heat exchanger

Fig. 8 shows the variation of SHE outlet temperature with heat exchanger effectiveness. As known, if the effectiveness increases, the heat exchange between the weak and strong solutions increases, and as a result of this, the temperature of the strong solution (T_9) decreases and that of the weak solution (T_7) increases. With an increase in the weak solution temperature entering the

generator, the heat load of the generator decreases. Similarly, with a decrease in the strong solution temperature entering the absorber, the heat rejected from the absorber also decreases. For this reason, decreasing ratios of both generator and absorber thermal loads increase with the effectiveness of the SHE (Fig. 9).

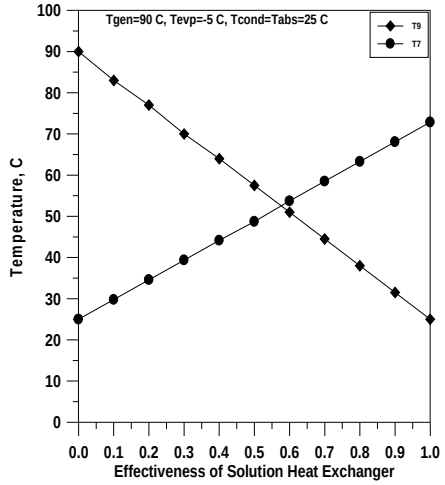

Fig. 8. Variation of solution temperature with the effectiveness of SHE

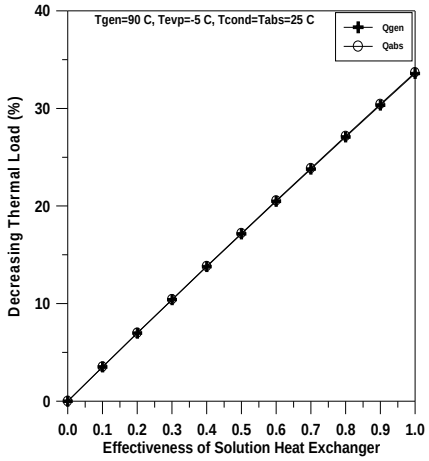

Fig. 9. Variation of decreasing thermal load with the effectiveness of SHE

The effects of the SHE on the system performance are given in Fig. 10. If the effectiveness of the SHE is zero ($\varepsilon_{SHE} = 0$), normally the COP increase ratio (PIR) is also zero. The performance of the system gets better with an increase in the effectiveness. For the best case condition ($\varepsilon_{SHE} = 1$, strong solution outlet temperature equals weak solution inlet temperature), the COP value increases up to a ratio of 50%.

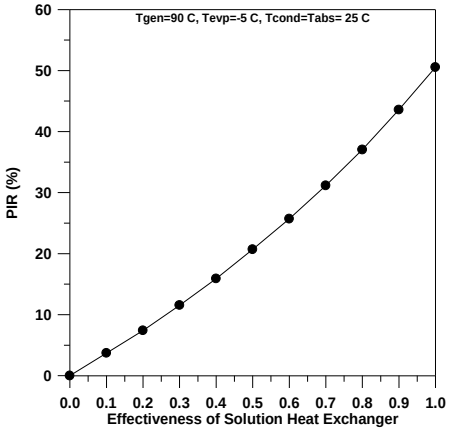

Fig. 10. Variation of PIR with the effectiveness of SHE

The variations of the coefficients of performance and efficiency ratio with the effectiveness of the SHE are shown in Fig. 11. While the COPc value does not change with the effectiveness and remains at 1.6, the COP value varies between 0.46 and 0.69. This means that the increasing ratio is about 50%, as given in Fig. 10. The COPc remains unchanged; the COP increases with effectiveness, and as a result of this, the η value increases (Fig. 11).

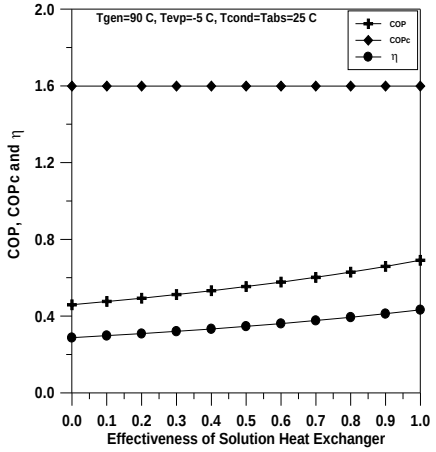

Fig. 11. Variation of performance parameters with the effectiveness of SHE

5 Conclusions

From the above study, the following results can be drawn:

• The thermal loads of the generator and absorber decrease, as the generator and evaporator temperatures increase. The decrease of the generator thermal load increases the COP value. Also, the COPc value increases with the generator and evaporator temperatures. Since the increase in the COP is greater than the increase in the COPc up to the generator temperature of 70 ^{o}C, the η value increases. When the generator temperature is above

70 ^{o}C, however, the COP increases and the η value decreases.

• The thermal loads of the generator and absorber increase as the condenser and absorber temperatures increase. The increase of the generator thermal load decreases the COP value. The COPc decreases with the condenser and absorber temperatures. The η value increases up to the condenser and absorber temperature values of about 40 ^{o}C, and then it decreases with higher temperatures.

• The increase of the SHE effectiveness decreases the generator and absorber thermal loads. The decrease ratio in the thermal loads of these components reaches 34%. As expected, the decrease in the generator thermal load leads to an increase in the performance and efficiency of system. The COP increases from 0.46 to 0.69 with use of the SHE. In this case, the maximum increase in the COP is 50%.

Notation

ARS	Absorption refrigeration system
COP	Coefficient of performance
CR	Circulation ratio
h	Enthalpy (kJ/kg)
$\dot{m}$	Mass flow rate (kg/s)
P	Pressure (kPa)
PIR	Performance increase ratio
Q	Thermal energy (kW)
SHE	Solution heat exchanger
T	Temperature (K)
X	Ammonia mass fraction in solution
W	Work input to pump (kW)

Greek

ε	Effectiveness of heat exchanger
η	Efficiency ratio of the system
v	Specific volume (m_3/kg)

Subscripts

abs	Absorber
c	Carnot
cond	Condenser
evp	Evaporator
gen	Generator
l	Liquid
me	Mechanical
v	Vapor
1....10	State points

References:

[1] Sierra, FZ., Best, R. and Holland, FA., 1993. Experiments on an absorption refrigeration system powered by a solar pond. *Heat Recovery Systems & CHP*, Vol. 13, pp. 401-408.

[2] Bulgan, A. T., 1995. Optimization of the thermodynamic model of aqua-ammonia absorption refrigeration systems. *Energy Conversion Management*, Vol. 36, No. 2, pp. 135-143.

[3] Sun, Da-Wen, 1998. Comparison of the performances of NH_3-H_2O, NH_3-$LiNO_3$ and NH_3-NaSCN absorption refrigeration systems. *Energy Convers. Mgmt*, Vol. 39, No. 5/6, pp. 357-368.

[4] Srikhirin P., Aphornratana S. and Chungpaibulpatana S., 2001. A review of absorption refrigeration technologies. *Renew Sust Energ Rev*, Vol. 5, pp. 343-72.

[5] Ben Ezzine, N., Barhoumi, M., Mejbri, Kh., Chemkhi, S. and Bellagi, A., 2004. Solar cooling with the absorption principle: first and Second Law analysis of an ammonia-water double generator absorption chiller. *Desalination*, Vol. 168, pp. 137-144.

[6] Jasim M. Abdulateef, Kamaruzzaman Sopian, M. A. Alghoul, Mohd Yusof Sulaiman, Azami Zaharim and Ibrahim Ahmad., 2007. Solar absorption refrigeration system using new working fluid pairs. *International Journal of Energy*, Vol. 1, Issue 3, pp. 82-87.

[7] ASHRAE, *ASHRAE Handbook, Refrigeration Systems and Applications*, Chapter 40, p. 40.1. ASHRAE, 1791 Tullie Circle, N. E., Atlanta, GA 30329, 1994.